

Manitoba's New Models for Correcting FWD Deflections to Standard Temperature for Pavement Design and Analysis

Principal Author:

M. Alauddin Ahammed, Ph.D. P. Eng.

Manager, Pavement and Materials Engineering Section
Manitoba Transportation and Infrastructure
1420- 215 Garry Street, Winnipeg, Manitoba R3C 3P3
Tel.: (204) 792 1338
Email: Alauddin.Ahammed@gov.mb.ca

Co-Authors:

Yasir Shah, P.Eng.

Pavement Design Engineer

Manitoba Transportation and Infrastructure
1420- 215 Garry Street, Winnipeg, Manitoba R3C 3P3
Tel.: (204) 791 2507
Email: Yasir.Shah@gov.mb.ca

Marcus Wong, P.Eng.

Pavement Assessment Engineer

Manitoba Transportation and Infrastructure
1420- 215 Garry Street, Winnipeg, Manitoba R3C 3P3
Tel.: (204) 792 9927
Email: Marcus.Wong@gov.mb.ca

Paper prepared for presentation
at the Innovations in Pavement Management, Engineering and Technologies Session
of the 2022 Annual Conference of the
Transportation Association of Canada
Edmonton, AB

Abstract

The load carrying capacities, relative strengths and the required overlays of existing pavements are generally determined using the measured surface deflection values. The Falling Weight Deflectometer (FWD) is the most common device for measuring pavement surface deflections. In all general pavement design and analysis, the measured deflection values are corrected to a standard effective pavement temperature. However, the effective pavement temperatures have been typically measured using an oil, poured into the predrilled holes on pavement surface. Such temperatures may not truly reflect the temperatures of pavement layers or materials. In addition, highway agencies typically apply a correction factor to central deflection only or apply a single temperature correction factor to all geophone deflections at a test point. These could result in some errors because of not accounting for the effect of temperature or lower sensitivity of farther (from FWD plate) geophone deflections to changes in temperature. Some jurisdictions, like Manitoba, also adopted the Benkelman Beam Rebound (BBR) deflections temperature correction models for FWD deflections. This may not be appropriate because of two different mechanisms of deflection measurement.

Manitoba Transportation and Infrastructure (MTI) has collected the temperature data from several thermistors to develop a new model for estimating the effective pavement temperature. The measured FWD deflections and temperatures at different sites were then used to develop a separate temperature correction model for each geophone deflection. The results and analyses showed that the estimated pavement effective temperatures using the new interim model are higher, with a smaller difference between the surface and effective temperatures, than that estimated using the currently used model. The correction model is different for each geophone deflection with a progressively smaller regression coefficient for geophones away (up to 900mm) from the centre of the FWD load plate. The new interim models also provide a reduction in the required overlay thickness.

Acknowledgement

The authors would like to acknowledge and thank the following staffs of MTI for their contribution in thermistor installation, thermistor and FWD data collection, data processing and preliminary assessment: Mobile Operations staffs, Andre Dupuis (Surfacing Program Manager), Gordon McNabb (Material Assessment Technologist), David Mandrick (Micro-surfacing Program Manager), Cole Adamson (Engineering Co-op Student), Ryan Thompson (Pavement Management Engineer). The authors would also like to thank Campbell Scientific for their technical assistance during thermistor installation.

Introduction

The load carrying capacity and the required overlay of a pavement depend on its structural strength including the subgrade stiffness, which are generally determined based on pavement surface deflection values. The relative strengths of different pavement sections are also typically determined through the measurement of pavement surface deflections. Numerous devices have been developed since the introduction of the Benkelman Beam, which measures the static rebound deflection of pavements. Over the last few decades, the FWD has become the device of choice for most highway agencies around the globe because the load application through FWD equipment most closely resembles the dynamic impact of a moving heavy vehicle on a pavement.

Most of the general pavement design and analysis methodologies have incorporated input parameters that are being estimated from the FWD deflection values. The estimation of these input parameters

require the measured deflection values be corrected (normalized) to a standard effective temperature and a standard load (or stress). The pavement temperature at 20mm below the surface or at the mid-depth of bound (e.g., asphalt concrete) surface layer is considered as an effective pavement temperature. During the day-to-day pavement surface deflection data collection, pavement surface and the ambient air temperatures are measured using thermometers (built-in with equipment or hand-held). A correlation model is used to estimate the effective temperature from the measured surface temperature. A temperature correction factor is then applied to the surface deflection values measured at varying temperatures to convert them to standard effective temperature, which is typically 20 °C (68 °F).

Different agencies or researchers have developed models for estimating the effective temperature from the pavement surface temperature. The effective temperatures were typically taken as the temperatures of an oil poured in predrilled holes into the pavement. Such temperatures may not truly reflect the temperatures of pavement layers or materials because of differences in thermal conductivities and environmental exposures. Several models are also available for estimating the correction factors, which can be used to convert the measured surface deflection values to values at the standard effective temperature. The available information indicates that the major focus of past works was on correcting the FWD central deflection values. As such, agencies typically apply a correction factor to the FWD central deflection value only or apply a single correction factor to all geophone deflection values at each FWD test point. These could result in some errors in the design and analysis because the effect of varying temperature on the FWD deflection basin are ignored or that the sensitivity of induced deflection to temperature progressively reduces with depth below the pavement surface. It should be noted that the deflections of farther geophones from the FWD load plate represent deflection of pavement at different depths below the surface. Some jurisdictions, like Manitoba, also adopted the temperature correction model developed for the BBR deflections for use with the FWD deflections. This could also be inappropriate because of two different mechanisms of deflection measurement. This study attempted to verify the past practice and to develop and use new models, if found to be appropriate, to normalize the FWD deflection values to the standard effective temperature for all applications in Manitoba.

Background

MTI has been collecting the BBR deflection data for pavement rehabilitation design, vehicle overweight impact assessment and spring weight restrictions until 2008. External Service Providers were engaged since 1992 to collect FWD deflection data from research sites and selected highway sections. With the acquisition of FWD equipment in 2008, MTI started gradual implementation of FWD deflection data in 2009 for all applications. MTI has been using the correlation shown below (Equation 1) to determine the effective pavement temperatures from the measured surface temperatures for asphalt concrete (bituminous) surfaced (flexible and composite) pavements [1]. For rigid and asphalt surface treated (semi-flexible) pavements, the effective temperatures are the same as the pavement surface temperatures.

$$T_{eff} = 1.5286 + 0.7476T_{surf} \quad (1)$$

Where,

$$\begin{aligned} T_{eff} &= \text{effective pavement temperature, } ^\circ\text{C} \\ T_{surf} &= \text{pavement surface temperature, } ^\circ\text{C} \end{aligned}$$

Based on Equation 1, the effective temperature is higher than the surface temperature when the surface temperature is 6.0 °C or below. At high surface temperatures, the differences between the surface and effective temperatures seem to be high; e.g., 8.6 °C difference when the surface temperature is 40 °C.

For all pavement assessment, design and analysis including the calculation of pavement layers and subgrade moduli, the measured deflection values from flexible, semi-flexible and composite pavements are normalized to a standard effective temperature of 20 °C (and standard stress of 566KPa, which equates to a 40KN load on a 30cm diameter FWD load plate). The correction factors are calculated using Equation 2 [2]. No temperature correction is required for the portland cement concrete (PCC) surfaced pavements.

$$CF = 10^{(0.0091*(20 - T_{eff}))} \quad (2)$$

Where,

CF = Correction factor for temperature
 T_{eff} = Effective pavement temperature in °C.

MTI has recently installed 13 thermistors on flexible pavements across the province to aid in various research work and the implementation of seasonal weights. Temperature sensors were installed in pavement layers and subgrade at different depths starting at 30mm and ending at 3.0m below the pavement surface. The recorded temperatures from some of these thermistors sites were used to develop a correlation model for estimating the effective pavement temperatures from the pavement surface temperatures. FWD deflection and pavement surface temperature data were then collected from several of these thermistor sites during different time of the day and different time of the year. The measured FWD deflection values and estimated effective temperatures were then used to develop a temperature correction model for each geophone deflection for flexible pavements. The newly developed and currently used models were then used to compare the corrected deflections, backcalculated subgrade modulus, effective structural number and required overlay as well as the total pavement thickness. This paper presents the details of this study, analysis and the resulting models.

Findings from Literature Review

The AASHTO 1993 [3] pavement design guide provides a chart of temperature correction factors for FWD central deflection (d_0) values to 20 °C (68 °F), which should be used for calculating the effective structural number (SN_{eff}). The chart includes lines for temperature correction factors for 50mm (2"), 100mm (4"), 200mm (8") and 300mm (12") thick AC layers, which are based on mid-depth temperature of AC layer and therefore, they vary depending on pavement thickness. However, AASHTO 1993 method did not include any temperature correction for the entire FWD deflection basin.

Lukanen et al. [4] used deflection and temperature data from 40 sites of the Long Term Pavement Performance (LTPP) program for improved prediction of temperature in asphalt pavement. The research developed a modified BELLS equation (Equation 3), called BELLS2. Correlations were also developed for estimating the normalized (to standard temperature) backcalculated modulus and correcting the deflection basin.

$$T_d = 2.78 + 0.912IR + \{ \log_{10}(d) - 1.25 \} * \{ -0.428IR + 0.533T_{1-day} + 2.63 \sin(hr_{18} - 15.5) \} + 0.0278IR \sin(hr_{18} - 13.5) \quad (3)$$

Where,

T_d = Pavement temperature at depth d, °C
 IR = Infrared surface temperature, °C
 \log = Base 10 logarithm

d = Depth at which mat temperature is to be predicted, mm
 T_{1-da} = Average air temperature the day before testing
 \sin = Sine function on an 18-hr clock system (with 2 radians equal to one 18-hr cycle)
 hr = Time of day, in 24-hr clock system, using 18-hour cycle

The recorded data in the above study showed some difference between the thermistor and manual (based on oil poured in pre-drilled holes). Application of the above model for a network or a long section of pavement covering a full day of data collection is cumbersome. Collection of site-specific maximum and minimum air temperatures for the preceding day is a challenge. Application of this model also may need local validation. The study also developed another model (BELLS3), shown below by Equation 4, for day-to-day use considering shading (sky cover) effect.

$$T_d = 0.95 + 0.892IR + \{\log_{10}(d) - 1.25\} * \{-0.448IR + 0.621T_{1-day} + 1.83 \sin(hr_{18} - 15.5)\} + 0.042IR \sin(hr_{18} - 13.5) \quad (4)$$

A study in Texas [5] indicated noticeable bias in BELLS2 model. Local calibration of the model showed improved prediction of temperature. A new alternate model (Equation 5), called Texas-LTPP equation, developed from the same data set, showed further improved prediction. The temperature variation with depth was shown to be linear.

$$T_d = 6.460 + 0.199(IR + 2)^{1.5} + \log_{10}(d) * \{-0.083(IR + 2)^{1.5} - 0.692 \sin^2(hr_{18} - 15.5)\} + 1.875 \sin^2(hr_{18} - 13.5 + 0.059 [T_{(1-day)} + 6]^{1.5}) - 6.784 \sin^2(hr_{18} - 15.5) * \sin^2(hr_{18} - 13.5) \quad (5)$$

A study in Tennessee [6] found that the BELLS3 equation accurately predict the mid-depth asphalt concrete temperatures below 25 °C. However, at temperatures above 25°C, the model under predicts the mid-depth asphalt concrete temperatures by approximately 5°C. The paper also indicted that for BELLS2 equations, the surface temperature was recorded after shading the asphalt surface for six minutes, which resulted in a bias. The one-minute shading time used in BELL3 equation also does not reflect modern day FWD equipment. The study developed an exponential function for temperature correction of backcalculated AC layer modulus. The model coefficients are site specific, i.e., a separate model is required for each project site.

Chen et al. [7] collected temperature and FWD data during later winter, spring and summer from four test sections with varying age in Texas. The temperatures of AC layer were recorded from thermocouples installed at 12.7mm below the surface, at mid-depth of AC layer and 12.7mm above the bottom of AC layer. The study concluded that temperature correction factor is not site dependent, but are pavement condition dependent (intact vs cracked pavements).

Transports Québec [8] uses the following equation (Equation 6) to estimate the temperature corrected AC modulus. The temperature at 2/3 depth of the AC layer is used as a reference temperature if thickness is known. Otherwise, temperature at 100mm and 60mm below the AC surface are taken as reference for highways and other roads, respectively.

$$E_1 = 10^{(4.05 - 0.016T)} \quad (6)$$

Where,

E_1 = Temperature corrected AC layer modulus at 20 °C, MPa

T = AC layer temperature, °C

Ilja Březina et al. [9] used pavement temperatures and FWD deflection data collected from 10 long-term monitored sections in the Czech Republic to develop regression curves for correcting the measured deflections and back-calculated elastic moduli to 20 °C. The temperature at 40mm depth was used in all analysis. Several regression curves were developed to represent different geophone deflections. The corrected deflection bowls were subsequently used as input for calculating the elastic modulus of pavement layers. The study concluded that the correction of deflection at sensors with spacing more than 900mm has a marginal effect. The elastic moduli of asphalt layers determined from uncorrected and corrected deflection bowls were similar for the majority of the tested sections.

Kim et al. [10] used data collected from four pavements in North Carolina with various types of layer materials and thicknesses to develop temperature correction procedures for deflections and backcalculated AC modulus. The study found that the AASHTO procedure produces significant errors in the corrected deflections. The new temperature correction procedure for deflections and backcalculated moduli were developed using mid-depth temperature of the AC layer as an effective AC layer temperature. The developed models for FWD deflection and AC modulus corrections are presented in Equations 7 and 8, respectively.

$$D_{68} = 10^{a(68-T)} * D_T \quad (7)$$

$$E_{68} = 10^{0.0153(T-68)} * E_T \quad (8)$$

Where,

D_{68} = Adjusted deflection to the reference temperature of 20°C (68°F)

D_T = Deflection measured at temperature T (°F)

$a = 3.67 * 10^{-4} * t^{1.4635}$ for wheel path and $3.65 * 10^{-4} * t^{1.4241}$ for lane center

t = Thickness of AC layer, in.

T = AC layer mid-depth temperature at the time of FWD testing, °F

E_{68} = Corrected AC layer modulus to the reference temperature of 68°F, ksi

E_T = Backcalculated AC layer modulus from FWD testing at temperature T, °F

Akbarzadeh et al. [11] summarized several correlations that were developed in different studies around the globe to estimate the temperature corrected AC modulus. The reference temperature varied from 15 to 25 °C at 1/3 depth from AC surface to bottom of the AC layer. C-LTPP [12] recommended drilling 50mm deep holes to measure the effective pavement temperature of AC layer using an oil.

The above literature review indicates a major focus on correcting the backcalculated modulus for temperature and limited focus on estimating the effective pavement temperature and temperature correction of the FWD deflections. The primary reason is the uncertainty associated with the prediction of effective pavement temperature. Manitoba uses the FWD deflection data for various purposes, including the implementation of spring weight restrictions. Manitoba is not yet using the backcalculated AC modulus for pavement rehabilitation design. The measurement of AC mid-depth temperature during day-to-day FWD testing is impractical and a safety hazard due to moving traffic. As such, Manitoba requires local models to predict the effective pavement temperature and correction factors for FWD deflections. This study is the first effort towards this goal.

Objectives and Significance

The objectives of the study are to:

- i. Verify the suitability of existing temperature correction models to Manitoba highways;
- ii. Develop local temperature correction models based on FWD deflections instead of BBR deflections and AC layer temperatures instead of temperatures of an oil; and
- iii. Continue to use the model parameters that are readily available for the ease of day-day use.

The objective of this paper is to share the results of this study and the developed models. The study results and new models may draw significant interest to agencies and researchers using the FWD deflections in pavement design and analysis.

Thermistor Sites and Temperature Data

In 2019 and 2020, MTI instrumented 13 existing asphalt pavements on different highway sections across the province with temperature and moisture sensors. The temperature sensors were in AC, granular base, subbase and subgrade layers. Figure 1 shows the locations of these thermistor sites.

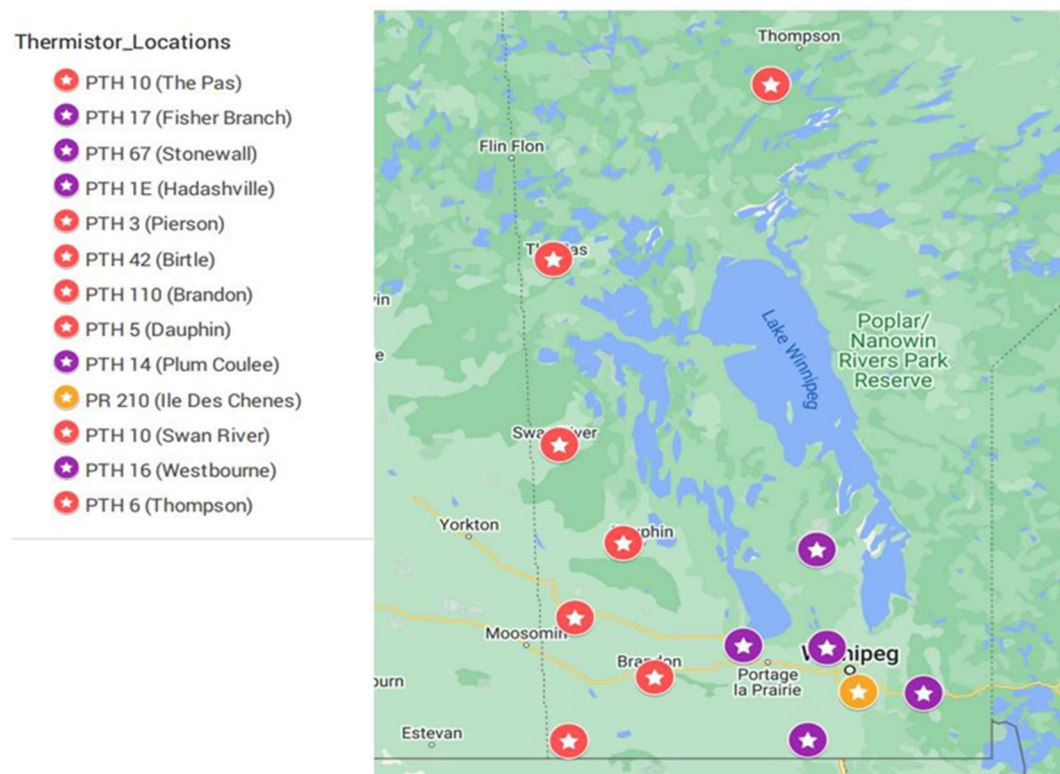


Figure 1. Thermistor site locations on Manitoba highways

Each thermistor installation consists of several external and internal temperature sensors (CS 231 SDI-12 Temperature Profiler) connected to a solar powered data logger. Depending on the thickness of the AC pavement, up to four (4) external sensors were installed in AC layer at 30mm, 50mm, 75mm and 125mm depths from the pavement surface. The internal sensors were sealed in a PVC tube. One external was

inserted or the first internal sensor was lined up at the AC and granular base layers interface. Sensors in the granular and subgrade layers were spaced depending on the thickness of the AC and granular layers with the last sensor being at 3.0m below the pavement surface. The thermistor holes were backfilled with sand. Five-star repair product was then used to surface the core location and fill the trench for cables.

Figure 2 shows the typical configuration of thermistor installation. A research-grade road surface infrared radiometer sensor (SI-4HR-SS: Research-Grade SDI-12) was installed on the roadside (data logger station) and pointed to the road surface to record the pavement surface temperature. An air temperature and relative humidity probe (CS 215-L) was also installed at the data logger station. All the data loggers were configured for recording the temperatures at 30 minutes interval.

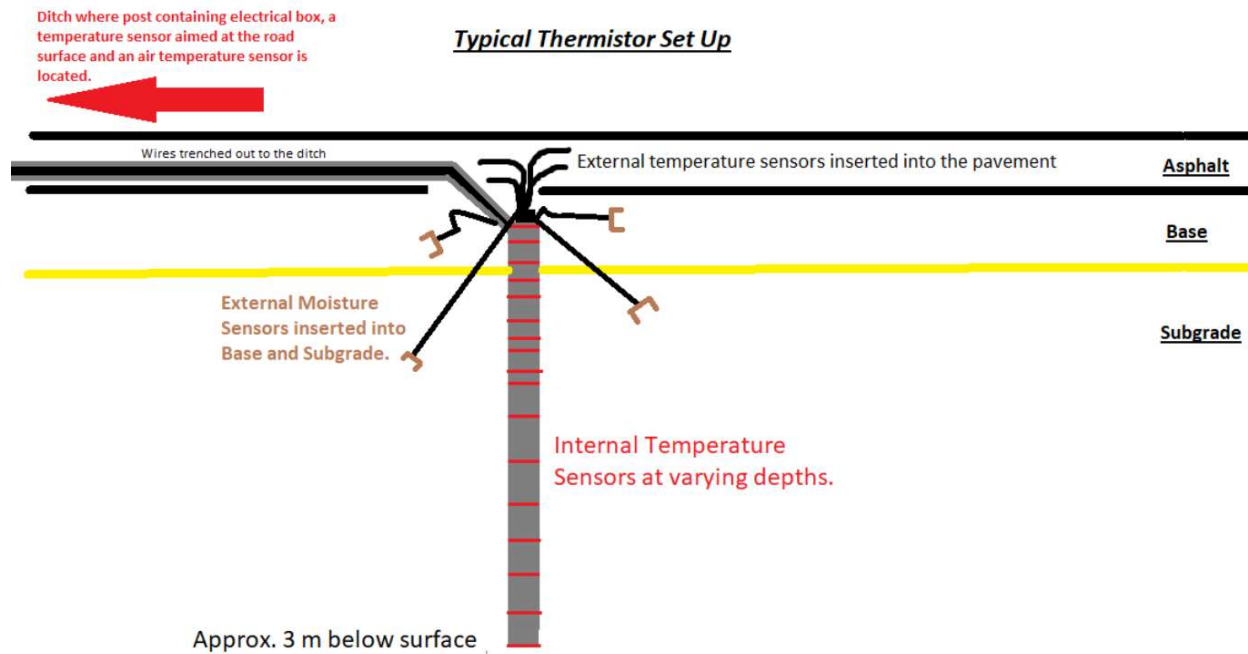


Figure 2. Typical layout of sensors for thermistor installation

Table 1 shows the pavement layers and subgrade information for the thermistor sites. As shown in the table, the AC thickness varied from 50mm (for thin surfaced) to 225mm and the granular layer thickness varied from 215mm to 675mm. The subgrade type varied from high plastic clay to fine sand.

Manitoba typically collects the FWD deflection data starting at three weeks after the removal of annual spring weight restrictions to ensure that pavements are at normal strength condition. The data collection typically ends when the ambient air temperature falls below 7 °C (which is typically in mid-October). Data are usually collected between 8:00 AM and 6:00 PM. To match with the standard FWD data collection protocol, temperature data recorded in 2020 between the above-specified time and mid-June to the end of September were retrieved from the complete dataset for this study. A random sample of data from the screened dataset was then used to develop the correlation between the pavement surface and effective pavement temperature. Any data with a rain event in the preceding 48 hours period were screened out to remove any associated bias. It should be noted that the effect of rain on the model for effective temperature was negligible in this study. Table 2 shows a sample of thermistor data used in this study.

Table 1. Thermistor sites pavement structure and subgrade data

Site #	Location	Layer Thickness (mm)			Subgrade Soil Type	
		Asphalt	Base	Total	AASHTO Class	Class Description
1	PTH 1E (Hadashville)	160	315	475	A-2-4	Fine Sand
2	PTH 67 (Stonewall)	200	280	480	A-7-6	High Plastic Clay
3	PTH 17 (Fischer Branch)	180	270	450	A-7-6/A-6	High/Low Plastic Clay
4	PTH 42 (Birtle)	90	240	330	A-7-6/A-6	High/Low Plastic Clay
5	PTH 3 (Pierson)	225	215	440	A-1-b/A-2-4	Coarse Sand/Fine Sand
6	PTH 10 (The Pas)	150	220	370	A-6/A-4	Low Plastic/Clayey Silt
7	PTH 14 (Plum Coulee)	165	675	840	A-7-6/A-6	High/Low Plastic Clay
8	PTH 5 (Near Dauphin)	185	355	540	A-7-6/A-6	High/Low Plastic Clay
9	PTH 110 (Brandon)	180	400	580	A-2-4	Silty Sand
10	PTH 16 (Westbourne)	160	360	520	A-4/A-6	Sandy Clay/Clayey Silt
11	PTH 10 (Swan River)	160	340	500	A-2-4	Fine Sand
12	PTH 6 (Paint Lake)	160	390	550	A-7-6	High Plastic Clay
13	PR 210 (Near PTH 59)	50	350	400	A-7-6	High Plastic Clay

Table 2. Sample of thermistor data (PTH 17, Fischer Branch)

Highway	Site Location	Date	Time	Air Temp., °C	Surface Temp., °C	Probe Temp. at 30mm, Deg. °C	Probe Temp. at 50mm, °C	Probe Temp. at 75mm, °C	Probe Temp. at 125mm, °C	Bit. Thickness, mm
PTH 17	Fischer	July 17, 2020	8:55:00 AM	22.22	24.6	24.38	24.07	23.34	23.31	180
PTH 17	Fischer	July 17, 2020	12:55:00 PM	22.9	25.86	28.7	28.63	27.66	25.72	180
PTH 17	Fischer	July 17, 2020	14:55:00 PM	23.22	28.18	29.78	29.38	27.87	26.16	180
PTH 17	Fischer	August 11, 2020	9:25:00 AM	20.24	25.91	23.35	23.03	22.41	22.76	180
PTH 17	Fischer	August 11, 2020	12:25:00 PM	23.75	35.29	32.01	30.98	28.16	25.47	180
PTH 17	Fischer	August 11, 2020	15:25:00 PM	24.76	37.59	36.37	35.51	32.73	28.99	180
PTH 17	Fischer	August 12, 2020	9:55:00 AM	24.22	28.99	25.62	25.09	23.82	23.38	180
PTH 17	Fischer	August 12, 2020	12:25:00 PM	26.26	37.28	32.88	31.87	28.93	26	180
PTH 17	Fischer	August 12, 2020	2:25:00 PM	27.65	39.8	36.83	35.74	32.48	28.48	180
PTH 17	Fischer	August 23, 2020	9:25:00 AM	19.82	26.19	23.4	23.12	22.78	23.25	180
PTH 17	Fischer	August 23, 2020	12:25:00 PM	20.8	27.65	26.84	26.59	25.79	24.84	180
PTH 17	Fischer	August 23, 2020	15:25:00 PM	24.68	36.39	30.48	29.79	27.83	25.95	180
PTH 17	Fischer	September 16, 2020	9:25:00 AM	5.805	8.81	10.09	10.03	10.46	11.75	180
PTH 17	Fischer	September 16, 2020	12:25:00 PM	8.09	18.76	16.91	16.17	14.58	13.37	180
PTH 17	Fischer	September 16, 2020	15:25:00 PM	9.44	20.15	21.4	20.69	18.91	16.33	180

FWD Data Collection and Processing

Five thermistor sites that are within driving distance from Winnipeg on a daily basis were selected for FWD deflection data collection. These sites are: i) PTH 17 (Fischer Branch), ii) PTH 14 (Plum Coulee), iii) PTH 67 (Stonewall), iv) PTH 16 (Westbourne), and v) PTH 1 (Hadashville). FWD data were collected from a 200m long section (100m on both sides of the thermistor location) at 10m interval (22 test points per site) for two or three cycles over the summer/fall months of 2020: August, September and November. Three rounds of FWD deflection measurements were taken in each particular day of data collection at a specific site during August and September: @8:00-10:00, @ 11:00- 12:00 and @15:00-16:30, depending on the ambient air and pavement surface temperatures. During the first week of November (because of cold October, but warm November), two or three rounds of measurements were taken from all sites, depending on the ambient air and surface temperatures, except PTH 17 for which no measurement was taken in November. At each test point, 40KN and 70KN loads (target loads) were applied to a 30cm diameter FWD load plate with two repeated drops of each load (i.e., four drops of loads at each test point).

Pavement surface and ambient air temperatures at each test point were recorded by an infrared thermistor installed with the FWD equipment. Surface temperatures were also recorded using a handheld laser thermometer to check the consistency of temperatures measured by the FWD mounted infrared

thermometer. Surface and subsurface temperatures during the FWD testing were also retrieved from the thermistor data loggers.

All the data were checked for consistency and reliability. It was noted that FWD readings from PTH 1 (Hadasville) site do not follow a logical or consistent trend for Geophone deflection at 600m, which is probably associated with subgrade type (sandy soil) and moisture condition or variation due to the presence of a roadside swamp. As such, PTH 1 site was excluded from further analysis.

The collected FWD deflection data were normalized to a standard 40KN load (566 KPa stress), which is one-half of the standard single axle load (corresponds to one equivalent single axle load), based on linear correlation between applied stresses and recorded deflections, and a simple average of all normalized deflections at each test point.

Thermistor Data Analysis and Model for Effective Pavement Temperature

Variation of Temperature with Depth

Figure 3 shows an example of the variation of pavement surface temperatures and the corresponding variation of pavement subsurface temperatures in AC layer for PTH 17 site. As shown in the figure, the surface and subsurface temperatures vary depending on the time of day and they do not follow a uniform or single straight-line trend. Many environmental parameters can cause instant variation of pavement surface temperature. However, there is always a time lag for a corresponding change in subsurface temperatures. The time lag also increases with subsurface depth. As a result, a nonlinear overall trend of pavement temperature profile in a pavement is a general phenomenon. Therefore, in the absence of any sensor at 20mm depth below the pavement surface, it was a challenge to determine the effective temperatures from the observed temperature profiles. Several trend analyses were completed and compared to determine the most suitable option for estimating the effective pavement temperatures from the pavement surface temperatures. Given the correlations between surface and subsurface temperatures at different depths are inconsistent, an interpolation between temperatures at pavement surface and 30mm depth below the surface was found to be the only feasible option for this dataset.

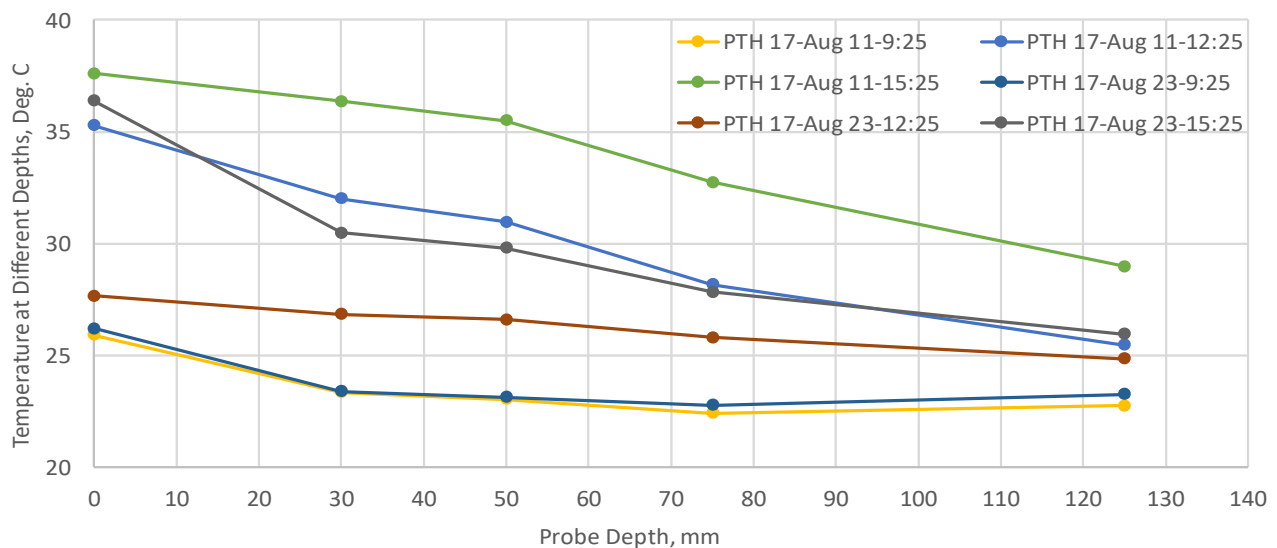


Figure 3. Variation of pavement surface and subsurface temperatures (Example, PTH 17)

Correlations between Surface and Subsurface Temperatures

Figure 4 shows the correlation, which represent the most practical trend, between temperatures at pavement surface and 30mm depth below the surface. The figure show a linear correlation between temperatures at pavement surface and 30mm depth below the surface. Figure 4 also shows some variances between the recorded surface and subsurface temperatures, with the subsurface temperatures being close to or above the surface temperatures at high surface temperatures, despite a good coefficient of determination value (R^2) of 0.84. These variances further emphasize the challenge of predicting the subsurface temperature from a single variable like the pavement surface temperature with 100% confidence. Manitoba is planning to collect additional data to confirm this trend and investigate for any possible issues related to sensors and/or the installation process.

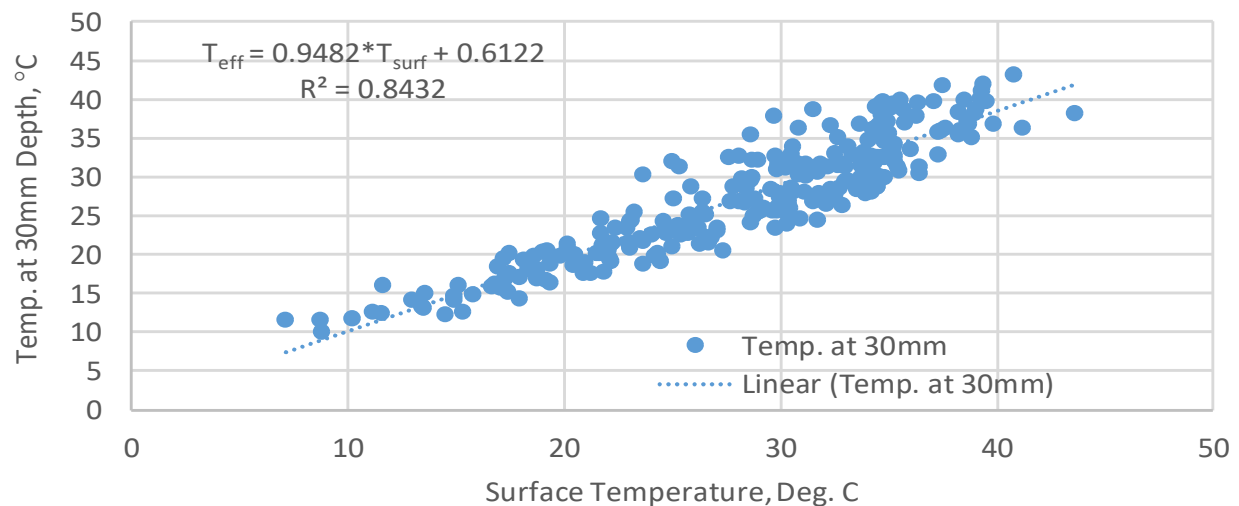


Figure 4. Correlation between temperatures at pavement surface and 30mm depth below the surface

Determination of Effective Pavement Temperatures

This study noted that the correlation between surface and subsurface temperatures varies depending on the season of the year and time of the day, making it more difficult to develop a universal model to estimate the effective pavement temperature that fits all seasons as well as time of the day and feasible to use on a day-to-day basis. Therefore, the interim model to estimate the effective pavement temperatures attempted to make a balance between the data needs for a more robust model, readily available data and ease of day-to-day application. The challenge was then to estimate the temperature at 20mm below the pavement surface given that a linear extrapolation from temperatures at 30mm and 50mm depth below the pavement surface was found to be unsuitable. As indicated earlier, based on the available data and model options, a linear interpolation between the temperatures at pavement surface and 30mm depth was found to be the only practical solution in this case. Figure 5 shows the correlation between interpolated temperature at 20mm depth (effective pavement temperature) and the pavement surface temperature. As shown in the figure, the correlation, with a R^2 value of 0.93, between the interpolated effective pavement temperature and pavement surface temperature is very good. Equation 9 shows the new (interim) model for estimating the effective pavement temperature.

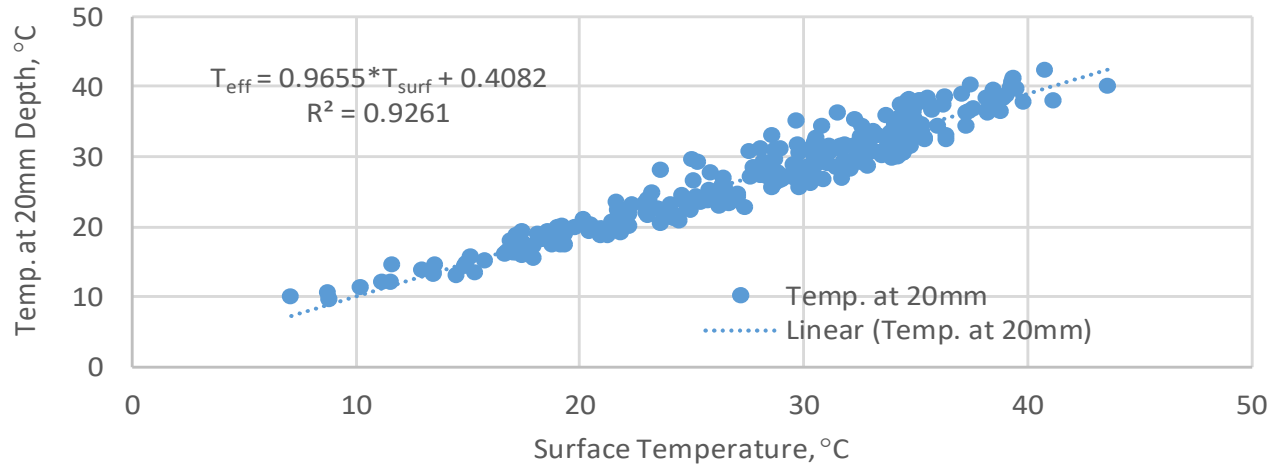


Figure 5. Correlation between effective pavement temperature and surface temperature

$$T_{eff} = 0.4082 + 0.9655T_{surf} \quad (9)$$

Figure 6 shows the variations of effective pavement temperatures at 20mm depth with the variation of pavement surface temperatures for the newly developed and the currently used models. As shown in the figure, when the surface temperature is lower than 11.8 °C, the new model provides higher effective temperatures than the surface temperatures. When the surface is warmer than 11.8 °C, the trend reverses to typical one with lower effective pavement temperatures than the pavement surface temperatures. This is slightly off from the currently used model, for which the break point is 6.1 °C. With the new model, the difference between surface and effective temperatures was also found to be smaller when it was compared with the currently used model. With the currently used model, the difference between the surface temperature and effective temperature seems to be unreasonably high, especially at high temperatures. For example, the effective temperature at 20mm depth below the surface is approximately 8°C lower when the surface temperature is 40 °C. Manitoba plans to further investigate and verify the predictions with additional and more detailed field data.

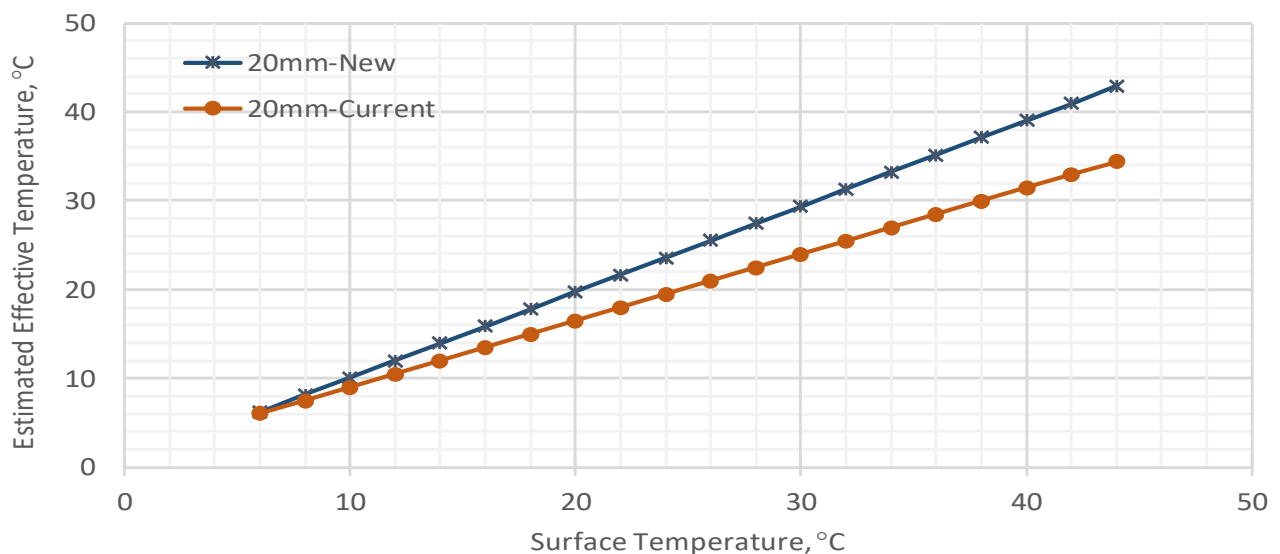


Figure 6. Variation of effective pavement temperatures with pavement surface temperatures

Verification of the Effective Temperature Model

The thermistor recorded surface and subsurface temperatures during the FWD deflection data collection were used to verify the interim model for estimating the effective pavement temperature. Since no temperature data at 20mm depth below the surface was available, the temperatures at 20mm depth below the pavement surface were estimated by interpolation from the recorded temperatures at the pavement surface and 30mm depth below the pavement surface in this case as well. Figure 7 shows the trend between the interpolated and model estimated effective temperatures. As shown in the figure, there is a good agreement between model predicted and interpolated effective pavement temperatures with an excellent R^2 value (0.98).

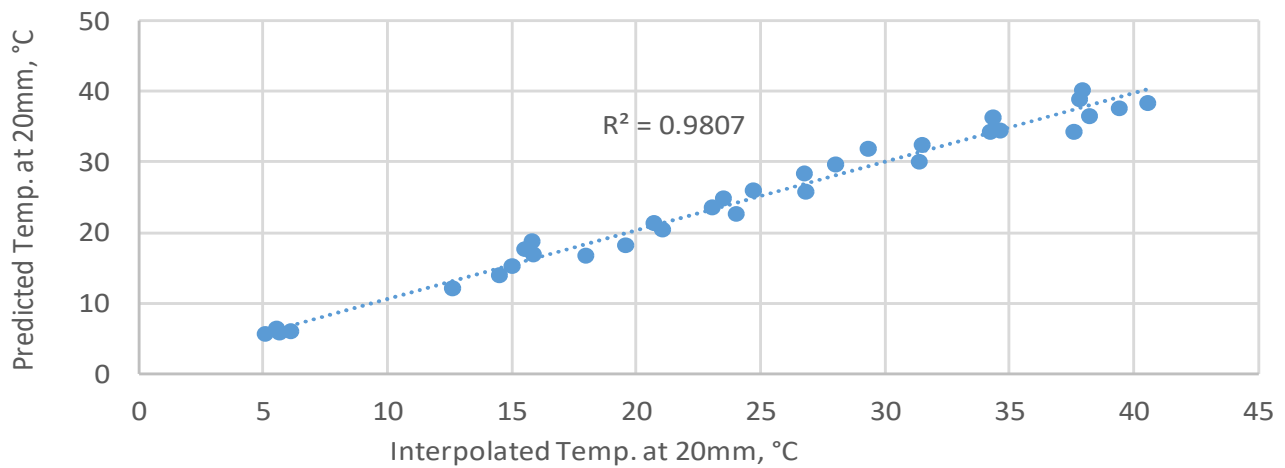


Figure 7. Verification of model for estimating the effective pavement temperature

FWD Data Analysis and Models for Temperature Correction

Effect of Temperature on Measured Deflections

To determine the correction factors for FWD deflections, the effective pavement temperatures (using the new model) for each deflection test point, at each of the four FWD deflection test sites, were estimated from the corresponding measured surface temperature. The analysis of the measured FWD deflection values and estimated effective pavement temperatures showed that correlation between the deflection and temperature is site specific. It depends on the pavement strength and temperature during the FWD deflection testing. The correlation also varies depending on the geophone position. Figure 8 shows examples (PTH 17) of correlations between geophone deflections and difference ($20 - T_{eff}$) of estimated effective temperatures (T_{eff}) from the standard effective temperature ($20\text{ }^\circ\text{C}$). As shown in the figure, the correlation varies depending on the geophone location, with a progressively weaker correlation for geophones further away from the FWD load plate.

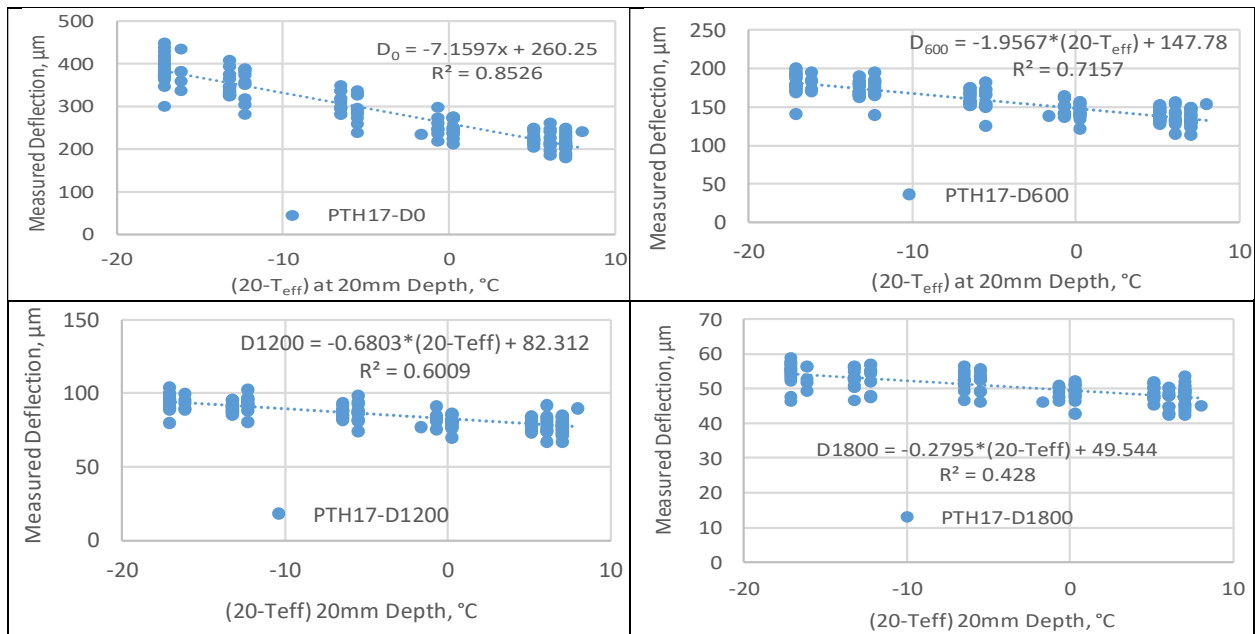


Figure 8. Example of temperature effect on measured geophone deflections

Due to the site and geophone specific variations of the effect of temperature on the measured deflections, each geophone deflections was plotted against the differences of standard and estimated effective pavement temperatures (20-T_{eff}) for each site. From the correlations between (20-T_{eff}) and the measured deflections, the deflection values corresponding to the standard effective temperature (20 $^{\circ}\text{C}$) were determined. Correction factors for each geophone deflections were then estimated by dividing the measured deflection values with the estimated deflections at the standard temperature. The correction factors for each geophone deflections were then plotted against the differential temperature (20-T_{eff}), after combing data from all four sites, to establish the best overall trend for each geophone deflections. Figures 9 and 10 show examples of trends for deflection correction factors for two geophone deflections. A logarithm function of the correction factors was found to be the best fit for estimating the deflection correction factors, and the trends were shown to vary depending on the geophone positions.

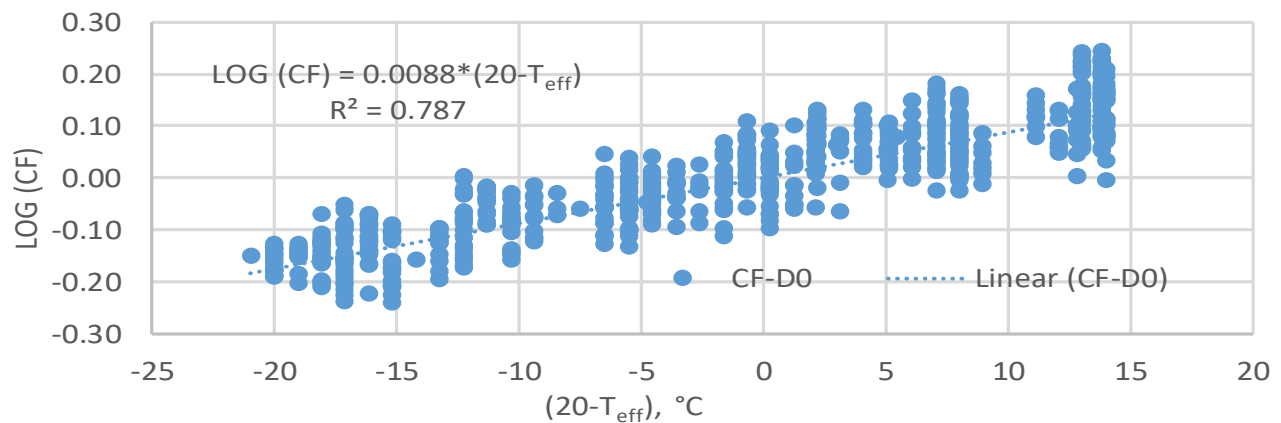


Figure 9. Trend of correction factors for FWD central deflections

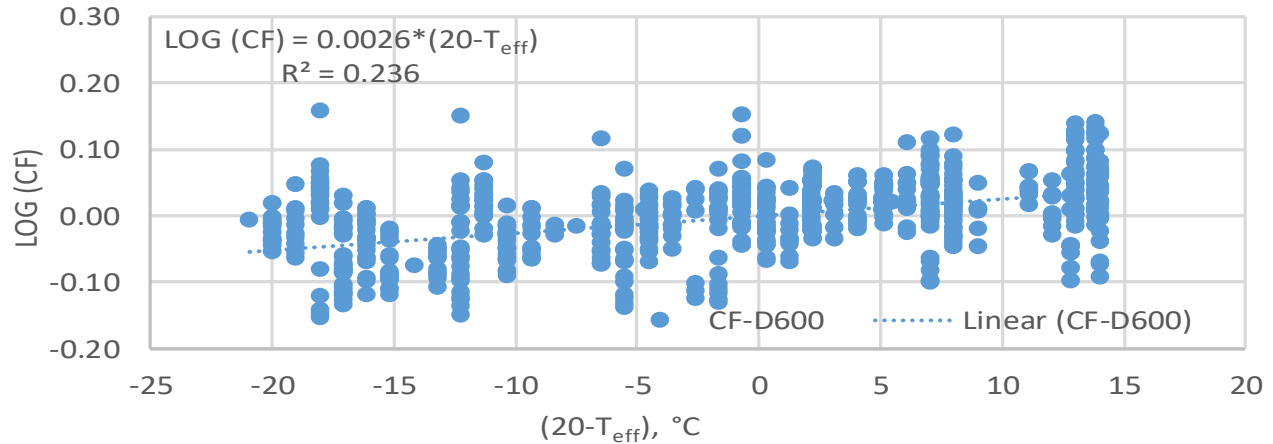


Figure 10. Trend of correction factors for geophone deflections at 600mm from FWD load plate

Models for Temperature Correction Factors

To develop a separate model for temperature correction factors of each geophone deflections, a linear regression analysis was done with differential temperature ($20 - T_{\text{eff}}$) as independent variable and the logarithm function of correction factors as dependent variable. The developed models, model statistics and ANOVA are presented in Table 3. As shown in the table, the models for deflection correction factors are different for each geophone deflections. The model coefficients become progressively smaller for further geophone deflections away (up to 900mm) from the centre of the FWD load plate. These lead to smaller correction factors for further geophone deflections when the effective temperature is less than 20 °C and larger correction factors for further geophone deflections when the effective temperature is higher than 20 °C as compared to the correction factors for deflections at the centre of the FWD load plate. The trend slightly reverses for further geophones with the same regression coefficients for geophones at 1500mm and 1800mm away from load plate. All models and model coefficients were found to be statistically significant at 95% confidence interval.

Table 3. Summary of models for FWD deflection correction factors

Geophone Location (mm)	Regression Statistics						
	Model	Adjusted R ²	Standard Error	# of Observations	Model Significance F	t- stat	p-value
0	$CF = 10^{0.0088 * (20 - T_{\text{eff}})}$	0.787	0.048259	658	1E-222	49.27552	8E-223
200	$CF = 10^{0.0062 * (20 - T_{\text{eff}})}$	0.651	0.047354	658	3E-152	35.02495	2E-152
300	$CF = 10^{0.0050 * (20 - T_{\text{eff}})}$	0.556	0.046945	658	8E-118	28.67243	7E-118
450	$CF = 10^{0.0034 * (20 - T_{\text{eff}})}$	0.354	0.048312	658	3E-64	18.96871	3E-64
600	$CF = 10^{0.0026 * (20 - T_{\text{eff}})}$	0.236	0.048188	658	2E-40	14.25329	2E-40
900	$CF = 10^{0.0018 * (20 - T_{\text{eff}})}$	0.146	0.046845	658	3E-24	10.59202	3E-24
1200	$CF = 10^{0.0019 * (20 - T_{\text{eff}})}$	0.176	0.044018	658	2E-29	11.84668	2E-29
1500	$CF = 10^{0.0021 * (20 - T_{\text{eff}})}$	0.210	0.041812	658	1E-35	13.23133	1E-35
1800	$CF = 10^{0.0021 * (20 - T_{\text{eff}})}$	0.193	0.044400	658	2E-32	12.53078	2E-32

$CF =$ Deflection Correction Factor for Temperature, $T_{\text{eff}} =$ Effective Pavement Temperature

Table 3 shows also that the model for central deflections is close to the currently used model (Equation 2). However, the currently used model does not appear to be applicable to other geophone deflections.

Effect of AC Layer Thickness on Temperature Correction Factors

Figure 11 shows the variation of correction factors for FWD central deflection with the variation AC layer thickness. It shows that the correlation between the deflection and AC layer thickness is weak. Single and multi-variables regression analysis including the effective pavement temperatures also shown that AC layer thickness is statistically insignificant for the estimation of FWD deflection correction factors, regardless of geophone positions.

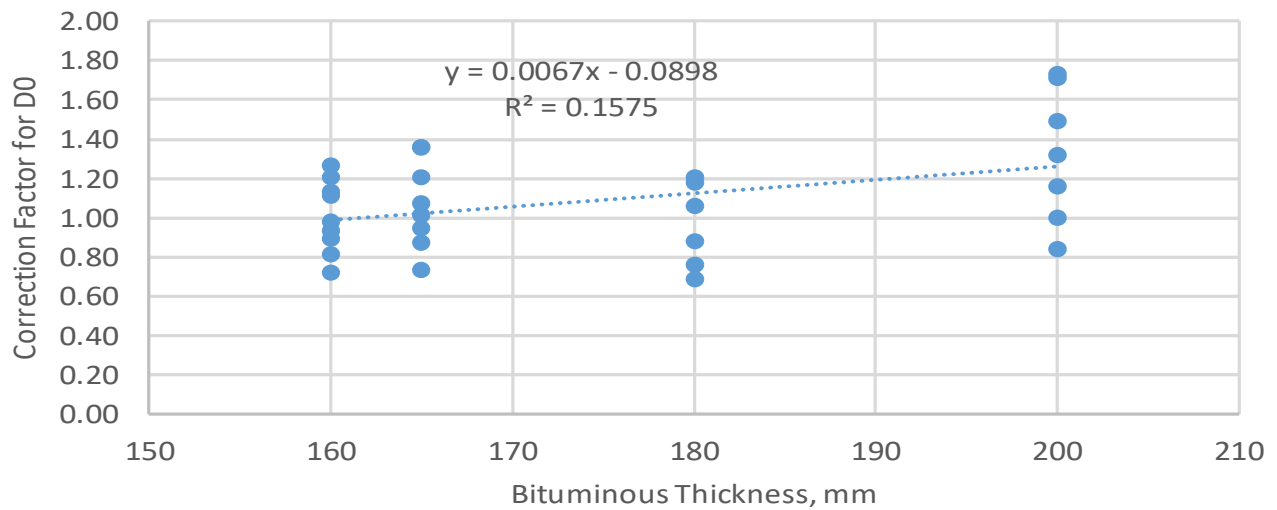


Figure 11. Effect of AC layer thickness on deflection correction factors (Example of central deflections)

Case Studies: Application of Temperature Correction Models

Comparison FWD Deflection Basins

The new temperature correction models were applied to FWD data from five highway sections. The bituminous thickness at these sites ranged from 50mm to 225mm, granular base thickness ranged from 100mm to 355mm and the measured surface temperature ranged from 2.8-39.1 °C. Figures 12 and 13 show examples of the variation of deflection basins for corrected with the currently used correction factors, newly developed correction factors and uncorrected values. Table 4 shows the summary of correction factors and deflection values with and without temperature corrections. As shown in the figures and table, the sensor position and surface temperature affect the shape of the deflection basins with the application of newly developed models. However, only temperature affect the deflection basin shape with the application of currently used models. Although the deflection basins matched each other when the effective temperature is 20 °C, the corresponding measured surface temperatures are 24.7 °C and 20.3 °C, using the current and new models, respectively.



Figure 12. Comparison of deflection basins for PR 352 @ Birnie at 3.6 °C

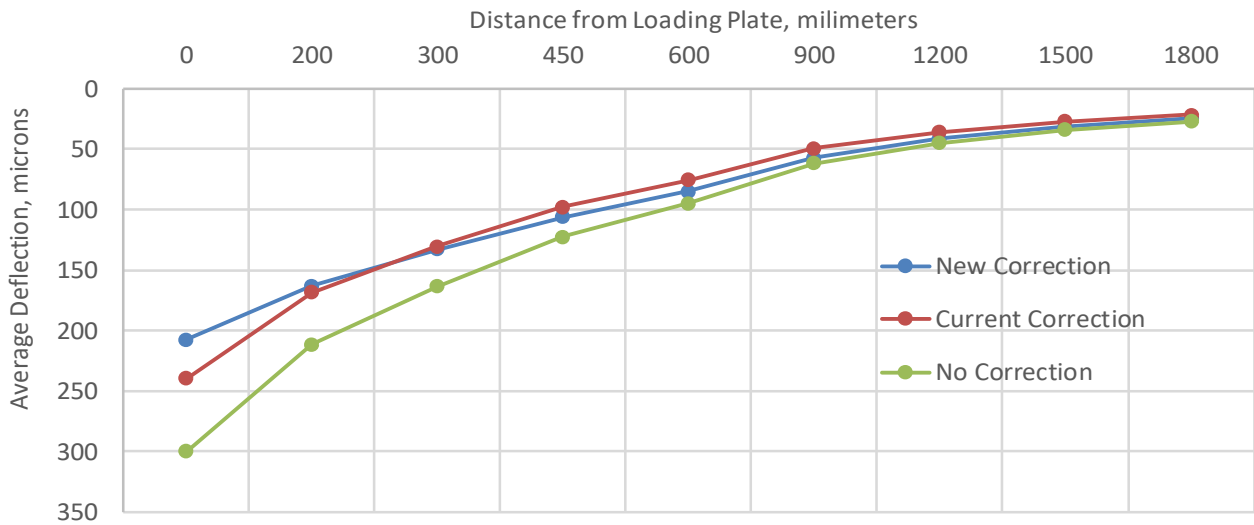


Figure 13. Comparison of deflection basins for PTH 3 (SK Boundary to PTH 83) at 39.1 °C

Effect of New Temperature Correction Models on Overlay Design

Table 5 shows examples of calculated effective structural numbers (SN_{eff}) for five sites. These examples show 5mm to 15mm savings in bituminous (AC) overlay thickness in rehabilitation design using the new effective temperature and deflection correction models.

Table 4. Comparison of correction factors and deflection basins

Highway	Section	Surface Temp., °C	Pvmt. Eff. Temp. (Current), °C	Pvmt. Eff. Temp. (New), °C	Sensor	Uncorrected deflection, μm	Correction Factor (Current)	Correction Factor (New)	Corrected deflection (New), μm	Corrected deflection (Current), μm
PTH 9	02009090HU	2.8	3.7	3.0	D0	412	1.408	1.411	580	580
					D200	360	1.408	1.274	457	507
					D300	321	1.408	1.216	389	452
					D450	263	1.408	1.142	300	371
					D600	219	1.408	1.107	243	309
					D900	156	1.408	1.073	167	219
					D1200	116	1.408	1.077	124	163
					D1500	88	1.408	1.086	96	124
					D1800	68	1.408	1.086	74	95
PR 352	02352050HU	3.6	4.2	3.7	D0	929	1.392	1.390	1293	1297
					D200	746	1.392	1.261	941	1041
					D300	600	1.392	1.206	724	838
					D450	425	1.392	1.136	483	593
					D600	302	1.392	1.102	333	421
					D900	180	1.392	1.070	192	251
					D1200	126	1.392	1.074	135	175
					D1500	96	1.392	1.082	104	134
					D1800	80	1.392	1.082	86	111
PTH 6	04006070HU	8.4	7.8	8.6	D0	121	1.290	1.260	152	156
					D200	101	1.290	1.177	119	131
					D300	89	1.290	1.140	101	115
					D450	74	1.290	1.093	81	95
					D600	62	1.290	1.071	66	80
					D900	45	1.290	1.048	47	58
					D1200	33	1.290	1.051	35	43
					D1500	26	1.290	1.057	27	33
					D1800	21	1.290	1.057	22	27
PTH 59	01059020HU	26.7	21.5	26.1	D0	687	0.969	0.883	606	666
					D200	500	0.969	0.916	458	485
					D300	372	0.969	0.932	347	361
					D450	255	0.969	0.953	243	247
					D600	183	0.969	0.964	176	177
					D900	110	0.969	0.975	107	106
					D1200	76	0.969	0.974	74	74
					D1500	57	0.969	0.971	55	55
					D1800	46	0.969	0.971	45	45
PTH 3	03003010HU	39.1	30.8	38.2	D0	300	0.798	0.692	208	239
					D200	211	0.798	0.771	163	169
					D300	164	0.798	0.811	133	131
					D450	123	0.798	0.867	106	98
					D600	95	0.798	0.897	85	76
					D900	62	0.798	0.927	57	49
					D1200	45	0.798	0.924	42	36
					D1500	34	0.798	0.916	32	27
					D1800	27	0.798	0.916	25	22

Table 5. Comparison of overlay AC thickness

Highway	Location	FWD Central Deflection, μm	Surface Temp., $^{\circ}\text{C}$	Effective Temp. (Current Model), $^{\circ}\text{C}$	Effective Temp. (New Model), $^{\circ}\text{C}$	S _{Neff} (Current Models), mm	S _{Neff} (New Models), mm	Overlay AC Thickness (Current Models), mm	Overlay AC Thickness (New Models), mm	Difference in AC thickness, mm
PTH 9	Winnipeg Beach	412	2.8	3.66	3.01	72.2	66.4	170	160	-10
PR 352	Birnie	929	3.6	4.20	3.74	38.9	35.4	202	190	-12
PTH 6	Eriksdale	121	8.4	7.84	8.60	140.8	136.0	39	28	-11
PTH 59	North of PR 201	687	26.7	21.51	26.12	31.9	35.1	185	180	-5
PTH 3	Pierson Thermistor site	300	39.1	30.77	38.18	96.1	106.6	54	40	-15

Effect of New Temperature Correction Models on Reconstruction Design

Table 6 shows examples of required layer thicknesses for five sites. These examples show up to 25mm savings in bituminous (AC) layer thickness in reconstruction design using the new effective temperature and deflection correction models at low and intermediate temperatures. At high temperatures, the required AC thickness is slightly higher when using the new models as compared to the current models. It should be noted these examples are intended to display the difference between the new and old models. In practice, an agency can increase, or decrease the thickness of AC, base and/or subbase layer(s) considering economy in construction and site constraints.

Table 6. Comparison of layer thickness for reconstruction

Highway	Location	FWD Central Deflection, μm	Surface Temp., $^{\circ}\text{C}$	Effective Temp. (Current Model), $^{\circ}\text{C}$	Effective Temp. (New Model), $^{\circ}\text{C}$	Effective Mr (Current Models), MPa	Effective Mr (New Models), MPa	Granular Base Thickness, mm	AC Thickness (Current Models), mm	AC Thickness (New Models), mm	Changes in AC Thickness, mm
PTH 9	Winnipeg Beach	412	2.8	3.66	3.01	16.0	20.4	500	162.6	137.6	-25.0
PR 352	Birnie	929	3.6	4.20	3.74	12.2	15.4	500	115.8	94.1	-21.7
PTH 6	Eriksdale	121	8.4	7.84	8.60	58.7	72.3	450	204.1	181.4	-22.7
PTH 59	North of PR 201	687	26.7	21.51	26.12	30.4	30.5	300	147.2	146.8	-0.4
PTH 3	Pierson Thermistor site	300	39.1	30.77	38.18	64.0	56.9	350	151.7	162.9	11.2

Concluding Remarks

The pavement temperature profiles vary widely depending on many ambient factors, which makes it difficult to predict the subsurface temperatures. The analyses and results show that the estimated pavement effective temperatures using the new interim model are higher, with a smaller difference between the surface and effective temperatures, than that estimated using the currently used model. At low surface temperatures up to 11.8 $^{\circ}\text{C}$, the effective pavement temperatures could be higher than the surface temperature, especially during fall. AC layer thickness was found to be insignificant for the estimation of FWD deflection correction factors, regardless of geophone positions.

The new FWD deflection correction factors vary depending on the measured surface temperatures and geophone locations. The new correction factors generally provide higher effective SN, which result in some reduction in overlay thickness. For reconstruction, the required pavement thickness is lower than

that using the current model when the measured temperature is less than about 27 °C. The trend reverses when the surface temperature is higher than 27 °C.

Future Work

Manitoba plans to collect additional data with more intensive data collection program to verify and finalize the developed models.

References

1. MIT 2007. *“Effective Pavement Temperature for the Normalization of Deflection Data From Benkelman Beam and FWD Tests”*. Manitoba Infrastructure and Transportation (MIT) Internal Report, February 2007.
2. Alberta Research Council 1975. *“Temperature corrections for Deflection Measurements in Flexible Pavements”*. Obtained through personal communication with Mr. Dave Hein, October 1999.
3. AASHTO 1993. *“AASHTO Guide for Design of Pavement Structure.”* American Association of State Highway and Transportation Officials, Washington, D.C.
4. Lukanen, E.O, Stubstad, R. and Briggs, R. 2000. *“Temperature Predictions and Adjustment Factors for Asphalt Pavement”*. Publication No. FHWA-RD-98-085, Federal Highway Administration, US Department of Transportation, McLean, VA.
5. Fernando, E.G., Liu, W. and Ryu, D. 2001. *“Development of a Procedure for Temperature Correction of Backcalculated AC Modulus”*. Report No. FHWA/TX-02/1863-1, Texas Transportation Institute, The Texas A&M University System, Austin, Texas.
6. Marshall, C., Meier, R. and Welch, M. 2001. *“Seasonal Temperature Effects on Flexible Pavements in Tennessee”*. Transportation Research Record 1764, Paper No. 01-3010, Transportation Research Board, Washington D.C.
7. Chen, D., Bilyeu, J., Lin, H. and Murphy, M. 2000. *“Temperature Correction on Falling Weight Deflectometer Measurements”*. Transportation Research Record 1716, Paper No. 00-1428, Transportation Research Board, Washington D.C.
8. St-Laurent, D. 2000. *“A simple rational approach for temperature correction of deflection basins.”* Presentation at 2000 FWD User’s Group meeting, Cornell University, Ithaca, New York.
9. Březina, I., Machel, O. and Zavřel, T. 2021. *“Temperature Correction of Deflections and Backcalculated Elasticity Moduli Determined from Falling Weight Deflection Measurements on Asphalt Pavements”*. University of Zilina, Transport Research Centre (CDV), Brno, Czech Republic, 2021.
10. Kim, Y. R., Hibbs, B. O., and Lee Y. 1995. *“Temperature Correction of Deflections and Backcalculated Asphalt Concrete Moduli”*. Transportation Research Record 1473, pp. 55-62, Transportation Research Board, Washington D.C.
11. Akbarzadeh, H., Bayat, A. and Soleymani, H. R. 2012. *“Analytical Review of the HMA Temperature Correction Factors from Laboratory and Falling Weight Deflectometer Tests”*. International Journal of Pavement Research and Technology, Chinese Society of Pavement Engineering, Vol. 5 No.1, pp. 30-39.
12. C-LTPP 1989. *“Pavement Research Technical Guidelines for the Falling Weight Deflectometer Testing”*. National Research Council, Ottawa, Canada.